Beginning of Exocytosis Captured by Rapid-freezing of *Limulus* Amebocytes

R. L. ORNBERG and T. S. REESE
Section on Functional Neuroanatomy, Laboratory of Neuropathology and Neuroanatomical Sciences, National Institutes of Health, Bethesda, Maryland 20205; and Marine Biological Laboratory, Woods Hole, Massachusetts 02543

ABSTRACT Structural changes underlying exocytosis evoked by the application of endotoxin to *Limulus* amebocytes were studied at the level of detail afforded by freeze-fracture and freeze-substitution techniques combined with the time resolution of direct rapid-freezing. The results with amebocytes prepared in this manner differed from those with other secretory cells prepared by conventional means. Exocytosis begins within seconds of endotoxin treatment when the plasmalemma invaginates to form pedestallike appositions with peripheral secretory granules. The juxtaposed membranes at these pedestal appositions form several punctate pentalaminar contacts, but examination of freeze-fractured pedestals failed to reveal any corresponding changes in the intramembrane particle distribution. Small secretory granule openings or pores, which are very infrequent, appear within the first 5 s after endotoxin treatment. These pores rapidly widen and this widening is immediately followed by the sequential dissolution of the granule contents, which then move into the surrounding extracellular space. Cytoplasmic filaments connecting the plasmalemma with the granule membrane are suitably deployed to be responsible for the plasmalemmal invaginations. How pores begin is not certain, but the appearance of clear spaces between the granule core and the granule membrane at this point in exocytosis supports the possibility of a role for osmotic forces.

Structural studies have contributed important ideas about the membrane rearrangements that underlie exocytosis. Indeed, the resolution of the electron microscope was required to show that the membranes of secretory granules are actually incorporated into the plasmalemma during an exocytotic event (28, 29). However, interpretation of structural data beyond this point is limited by the poor time resolution inherent in chemical fixation as customarily used to prepare tissues for electron microscopy. Exocytosis evoked by fixation (10, 38) has not been found in most secretory cells, but exocytotic openings of secretory granules in cells stimulated before or during chemical fixation are so frequent that it is necessary to conclude that these events are slowed to the point where they are collected over periods of activity lasting several seconds (12, 39). The alternative possibility, that each exocytotic event actually lasts several seconds, is less likely because direct observation of secretion in living cells indicates that individual exocytotic events last less than a second (34).

Secretion at *Limulus* amebocytes was studied using direct rapid-freezing to decrease distortions in the time-course of exocytosis. This was made possible by a rapid-freezing method that, with minimal ice-crystal damage, "cryofixes" the surface of the tissue in a few milliseconds instead of the seconds required by aldehyde fixatives (11). Indeed, the number of exocytotic events that accompany a single burst of secretion in nerve-muscle synapses prepared by this method corresponds exactly with the number of physiologically monitored secretory events or quanta (11).

Distortion of the time-course of exocytosis is not the only reason to resort to rapid-freezing. Structural changes that are not part of exocytosis as it occurs under normal circumstances may be induced by chemical fixatives. In particular, rearrangements of intramembrane particles where secretory granules contact the plasmalemma have been reported in a variety of secretory systems prepared by conventional methods (24). However, in a recent study using sea urchin eggs, the rapid-freezing method failed to reveal these particle rearrangements (3).

The observations presented here are based on rapid-freezing of *Limulus* amebocytes at rest and after secretory stimulation in order to examine the initial stages of exocytosis in the absence of time distortions or artifacts associated with ordinary

THE JOURNAL OF CELL BIOLOGY · VOLUME 90 JULY 1981 40-54
© The Rockefeller University Press · 0021-9525/81/07/0040/15 $1.00

preparatory methods. We hoped to see what new structural details surrounding the initiation of exocytosis appear with the millisecond time resolution of the rapid-freezing method. We did not intend to explore the effects of aldehyde fixatives; this has been done in other systems (3). A recent study using rapid-freezing to stop secretion in mast cells has yielded freeze-fracture views of the early stages of exocytosis similar to those presented here (4).

Our earlier observations based on freeze-etching (26) are extended here to include an examination of thin sections of cells frozen during exocytosis and prepared by freeze-substitution. Examination of such thin sections overcomes certain inherent difficulties of freeze-etch views in defining exact relationships between the granule and plasma membranes. Furthermore, observations on thin sections of fixed cells have been the basis for the important concept that membrane fission leading to exocytosis is preceded by fusion of the granule membrane with the plasma membrane (7, 29). The applicability of these concepts and the accuracy with which they describe exocytosis in *Limulus* amebocytes are examined here.

MATERIALS AND METHODS

Adult male horseshoe crabs *Limulus polyphemus* were obtained from the Marine Biological Laboratory, Woods Hole, Mass. Endotoxin from *Salmonella typhosa* 0906 or *Escherichia coli* B-12 was purchased from Difco Laboratories, Detroit, Mich., and dissolved in amebocyte Ringer's solution to a final concentration of 4 mg/ml. This amebocyte Ringer's, formulated to match the ionic composition of *Limulus* plasma (35), contained 454 mM NaCl, 10 mM KCl, 10 mM $CaCl_2$, 32 mM $MgCl_2$, 14 mM $MgSO_4$, and 20 mM HEPES buffer, pH 7.8. Endotoxin-free Ringer's was made by baking preweighed salts overnight at 180°C and dissolving them in triple-distilled water. All glassware was also baked overnight at 180°C and only pyrogen-free, disposable syringes and hypodermic needles were used. These procedures were required to avoid inadvertently stimulating the cells to secrete as they were withdrawn from the crab. Cytochalasin D (Sigma Chemical Co., St. Louis, Mo.) was diluted from a stock solution of 1 mg/ml in ethanol into cell-free *Limulus* plasma to a final concentration of 10 μg/ml. For the fixative experiment, 3% glutaraldehyde and 2% formaldehyde in *Limulus* Ringer's was prepared just before use.

Rapid-Freezing

Amebocytes were frozen by pressing them against a copper block cooled with liquid helium (11). Amebocytes were withdrawn from blood cavities in the heart or tibial leg segments into 1-ml syringes through 20-gauge needles. The soft skin covering the joints between the carapace and abdomen, or at the leg joints, was first rinsed with 70% ethanol and each area was punctured only once in any animal. To study endotoxin-stimulated amebocytes, a syringe containing 0.5 ml of blood was attached immediately to a T-adapter to which was also connected a 100-μl syringe filled with endotoxin-containing Ringer's. By simultaneous ejection from both syringes, blood containing amebocytes was rapidly mixed with endotoxin solution and expressed through a fresh 20-gauge needle. Several drops were discarded before a single drop of the blood-endotoxin mixture was put on a circle of Whatman #32 filter paper glued to an aluminum specimen support and rapidly frozen. The typical time from puncture to placing the blood on the specimen support was 10–15 s. The shortest possible interval or stimulus time between mixing amebocytes with endotoxin-containing Ringer's and freezing by contact with the cold copper block was 1 s.

Unstimulated amebocytes were prepared by freezing cells (*a*) directly after withdrawal from a crab at room temperature, (*b*) after withdrawal at room temperature and mixing with endotoxin-free Ringer's, and (*c*) directly after withdrawal into cold syringes from crabs cooled to 2°–4°C in chilled seawater. For the cytochalasin D experiments, 3 ml of *Limulus* blood was withdrawn into a syringe containing 5 μg of cytochalasin D in *Limulus* plasma, using ethanol in plasma for a control. The amebocytes were held in this solution for 5–10 min before use.

Freeze-Etching

Frozen amebocyte samples were freeze-etched in a Balzers 301 apparatus (Balzers Corp., Hudson, N. H.). The transfer of specimens onto the specimen cold stage and the procedures for fracturing them with the microtome have been described (11). Specimens were fractured at −110°C (nominal), etched for 1–5 min, and then shadowed unidirectionally or during partial rotation with 2–3 nm of platinum measured with a quartz crystal monitor. The freeze-etch micrographs are presented in the form of negative prints, i.e., platinum deposits are white and the shadows are black.

Freeze-Substitution

Rapid-frozen amebocytes were freeze-substituted in acetone (spectrophotometric grade; Aldrich Chemical Co., Inc., Milwaukee, Wis.) containing 4% osmium tetroxide. Just before use, 1 g of osmium tetroxide was dissolved in 25 ml of acetone. Equal amounts of this mixture were poured into four polyethylene scintillation vials and then immediately immersed and frozen in a liquid nitrogen bath. To each vial was added 10 ml of liquid nitrogen and then one amebocyte specimen, cell side up and still attached to the aluminum specimen support disk. The vial was then placed in a rack inside a double-walled, insulated container containing liquid nitrogen. The container was gently rotated and allowed to warm passively to room temperature. The warmup was recorded from a dummy substitution vial containing a thermocouple submerged in acetone. The substitution time, beginning when the acetone melted at −95°C and ending when room temperature was reached, was typically 9–12 h.

After an additional 1–2 h at room temperature, the amebocyte preparations were washed with three changes of acetone for 20 min each and stained with 0.1% hafnium tetrachloride (Alpha Scientific Inc., Hayward, Calif.) in acetone for 3–4 h at room temperature, as suggested to us by Dr. Morris Karnovsky, or with a saturated solution of uranyl acetate in methanol at 4°C. Hafnium staining was followed by three washes with acetone followed by two washes with methanol of 20 min each (to wash out salts that interfere with embedding). The amebocytes were then flat-embedded in Araldite (CY212); the aluminum specimen support was removed only after the Araldite was polymerized. Series of 20–60 thin (40–50 nm) sections were cut from well-frozen areas in the center of the block, picked up on Formvar-carbon-coated slot grids, and stained with 8% uranyl acetate in 50% methanol for 30–45 min followed by Reynold's lead citrate for 2–5 min. Replicas and stained thin sections were examined at 100 kV in either a JEOL 100 CX or an AEI-802 electron microscope equipped with 60° tilt stages; stereo pairs were tilted 8–10°.

RESULTS

General Properties of Amebocytes

Amebocyte blood cells from horseshoe crabs offer a number of advantages for studying exocytosis by quick-freezing. First, ice-crystal damage to cells within the first 20 μm of the frozen specimen surface is negligible. This region of good freezing is deeper than in many other tissues, presumably because of the high concentration of solutes in *Limulus* blood (27). Second, in confirmation of previous reports (18), amebocytes are the only type of cell observed in the blood and are present in sufficient concentration in the late summer and fall (2×10^6 cells/ml) to eliminate the need for isolation procedures common for other secretory cell preparations. Finally, amebocytes are extremely sensitive to endotoxin, and most cells degranulate within 30 s of endotoxin application (Figs. 1 and 2). This rapid rate of secretion affords a sufficient degree of synchronization among amebocytes to yield a workable number of transient morphological changes during the few milliseconds required to complete freezing.

The synchrony of exocytotic events achieved by this approach allowed the state of exocytosis in the most progressed cells to be correlated with time of exposure to endotoxin, even down to the shortest stimulation period of 1 s. Thus, cells from preparations stimulated for <5 s exhibited the prodromata of exocytosis. At 5–10 s, small exocytotic openings connected peripheral granules with the extracellular spaces in many cells. Later, between 10 and 15 s, most peripheral granules and many internal granules had undergone exocytosis. In the present study, we have limited our observations to a description of the morphological changes occurring in connection with exocytosis of the peripheral granules at intervals between 1 and 15 s after

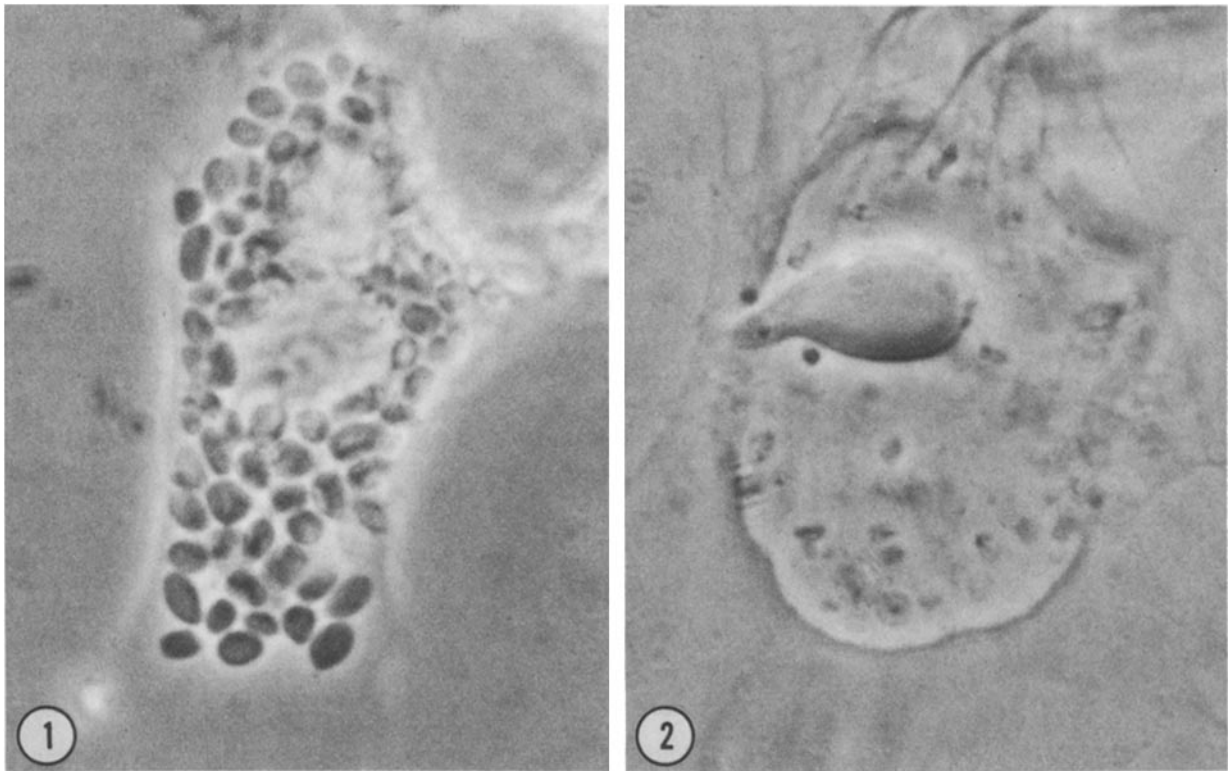

FIGURES 1 AND 2 Amebocyte attached to glass slide before (Fig. 1) and after (Fig. 2) application of endotoxin. The secretory granules in this cell were discharged within 30 s after secretion started. × 1,000.

application of endotoxin.

In addition to their secretory activity, amebocytes have motility and aggregation functions stimulated by their withdrawal from the crab (17, 18). However, corresponding formation of microspikes and pseudopods was not prominent until 30–45 s after withdrawal, which is later than the time intervals considered here. Furthermore, three sets of unstimulated control cells—cold cells, quickly drawn cells, and cells mixed with endotoxin-free Ringer's for 1–15 s—did not differ in their surface morphology. These controls gave us confidence that the morphological changes that appear after 1–15 s of exposure to endotoxin do not constitute reaction of a motility or aggregation system to mechanical stress or other factors that might accompany withdrawal or the rapid-mix stimulation technique.

Amebocytes Examined with Freeze-Fracture

Fracture faces of amebocytes from control experiments had smooth contours, and the intramembrane particles on both faces exhibited a range of sizes. Unlike the situation in most cell membranes, many large particles ($42/\mu m^2$) stood out on external plasmalemmal leaflets but were rare on cytoplasmic plasmalemmal leaflets (Figs. 3–8, and 11). Deep surface invaginations, 50–100 nm in diameter, often cross-fractured at their apices, were identified as coated pits in thin-section views of freeze-substituted cells. The coated pits were clustered unevenly over the cell surface and consequently were found in a disproportionately small fraction of the fractured amebocytes. This distribution and frequency, so far as we could tell from inspecting replicas, did not change during the short periods of endotoxin stimulation used in the present experiments. Therefore, the coated pits are not considered further here.

Striking changes did occur in the surfaces of cells exposed to endotoxin. Plasmalemmal bulges, ~0.25 μm in diameter, protruding from the cell surface were one of the first signs of endotoxin stimulation (Fig. 4). The bulged plasmalemma had a normal particle distribution on both fracture faces, and two or three bulges were frequently aligned in closely spaced rows. Rare cross-fractures through these bulges showed that they are associated with swelling of subsurface endoplasmic reticulum, and thin-section views of freeze-substituted cells confirmed this conclusion. Examination of these cisterns with a microprobe suggests that they contain large concentrations of calcium after they swell; this finding will be described in more detail in a later paper, so it will not be considered further here. Control preparations rapidly mixed with endotoxin-free Ringer's either did not show these changes or, in a few instances, showed them only to a minimal degree.

The remaining changes in the cell surface after endotoxin treatment represent plasmalemmal involvement in granule exocytosis. These changes consisted of: inward depressions of the plasmalemma to contact secretory granules, the formation of a pore within these depressions, and the subsequent widening of this pore. This sequence of plasmalemma-granule interaction seems to be more rapid than the synchronization between cells in the same experiment, because the similarity of the stages seen within the same cell was greater than that between different cells from the same experiment. Our attempt at sequencing these stages is therefore based on changes in the proportion of cells showing a particular stage in exocytosis, and on a steady progression of new stages after different periods of exposure to endotoxin from 1 to 15 s.

Inward bulges or depressions of the plasmalemma appeared 1–5 s after endotoxin treatment concomitant with the outward bulges caused by swelling of endoplasmic reticulum (Fig. 4).

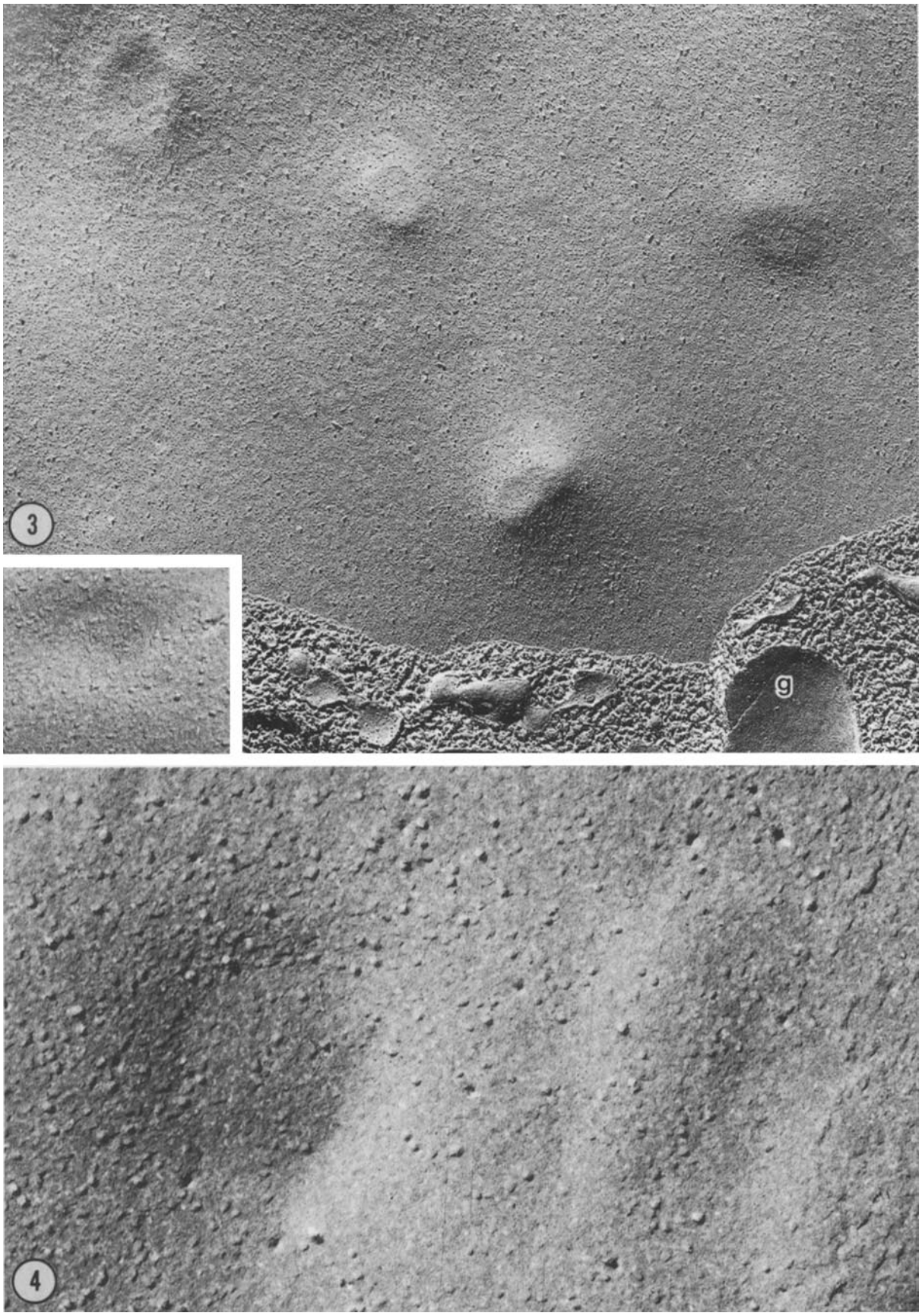

FIGURES 3 AND 4 Typical features of E-(Fig. 3) and P-(Fig. 4) fracture faces of amebocytes stimulated for short times (1–5 s) with endotoxin. Inward bulges of the plasmalemma with flat or outwardly curved tops have approximately the same spacing as the secretory granules (g) inside the cell. Outward bulges with rounded tops (on right side of Fig. 4) also appear during stimulation; these bulges correspond to displacement of the plasmalemma by swollen subsurface cisterns of endoplasmic reticulum. The distribution of intramembrane particles on both types of bulges is similar to that on the rest of the plasmalemma. *Inset*: P-fracture face of stimulated amebocyte prepared with aldehyde fixation. Fig. 3, × 50,000; Fig. 4, × 200,000; *inset*, × 70,000.

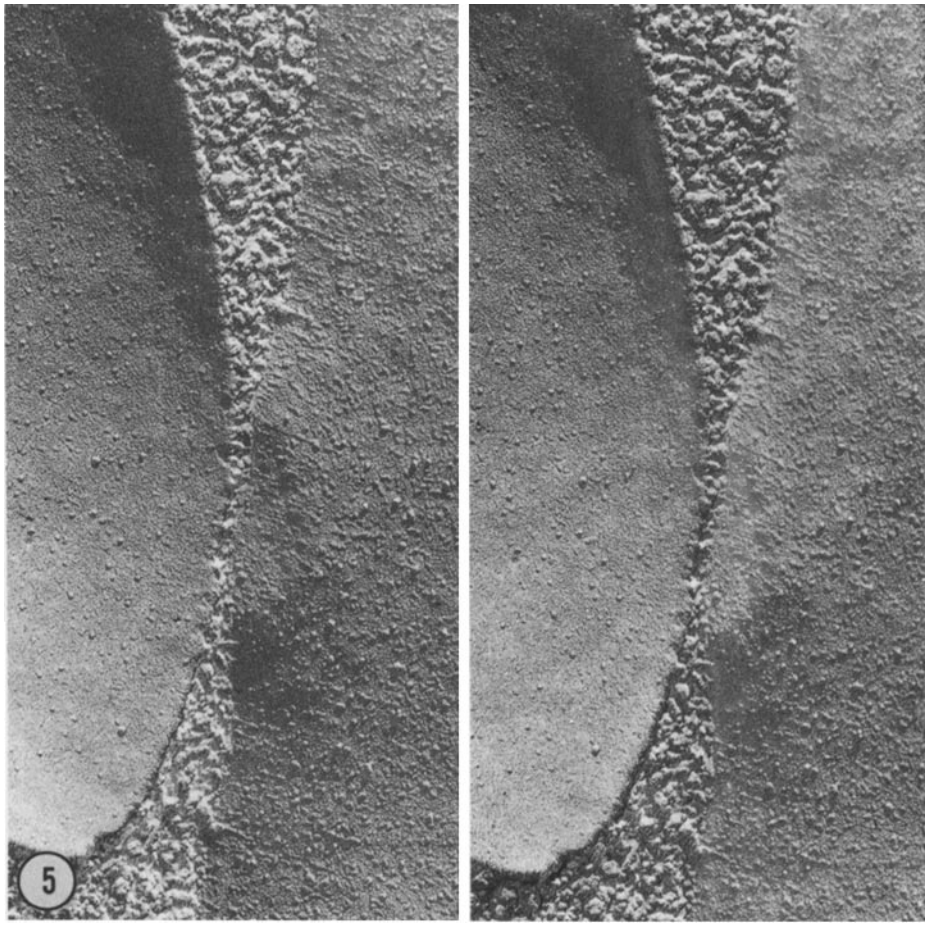

FIGURE 5 Stereo micrographs to show relationship of the inward type of bulge to a secretory granule. The E face of the bulge (right) forms a pedestal where the overlying secretory granule's P face (left) apposes the plasma membrane. Such appositions cause the flat or outwardly curved tops of pedestals. × 45,000.

Early forms of these plasmalemmal depressions were shallow, hyperbolic domes ~0.25 μm in diameter (Fig. 6). Coated pits, in contrast, had steeper sides and more deeply invaginated the cell surface (not shown) though this distinction was by no means clear in every instance. By 5 s, the majority of early forms had widened into shallow, circular depressions with flat or slightly concave bottoms (diameter, 0.3 μm ± 0.14 SD; n = 26; Figs. 3–6). Views of fortuitous cross-fractures through early forms showed that they are pedestals where secretory granules contact the plasmalemma and that the flat or concave apices of these pedestals are appositions with secretory granule (Fig. 5). Consistent with this interpretation, the spacing between pedestals was typically the diameter of a secretory granule (Figs. 3 and 6).

There were no obvious differences in the sizes or distributions of particles on the plasmalemmal fracture face between those regions of the membrane forming the top of a pedestal and the rest of the plasmalemma (Figs. 3–7). We looked for a difference by counting the large particles on E faces at the tops of and beside pedestals in 26 examples but did not find a significant difference in their concentration at these two locations. For comparison of fixed and directly frozen cells, the blood-endotoxin mixture was dropped directly into glutaraldehyde in *Limulus* Ringer's. Pedestals with particle distributions identical to those in directly frozen cells were present, but the extensive examination required to find subsequent steps in exocytosis similar to those found in directly frozen cells was not performed (Fig. 3, *inset*).

Two pedestals from ~500 freeze-fracture views frozen within 1–5 s after addition of endotoxin had small pores at their apices. The smallest of these pores had an elliptical shape with axes of ~10 × 40 nm (Fig. 7). Wider openings, 150 nm or more in diameter, were much more frequent and a few fortuitous cross-fractures showed that some were exocytotic openings, where the plasmalemma was connected to the granule lumen by a narrow neck (Figs. 8 and 9). The very low frequency of small pores compared with the abundance of wider ones, even from the same experiment, suggests that the radial expansion of a pore is very rapid. Confirmation that these pores are openings of secretory granules was obtained in thin-section views of freeze-substituted cells as discussed below. Large pores were sufficiently frequent for this point to be confirmed in freeze-fractured amebocytes (Figs. 8 and 9).

We found no distinctive differences in the distribution of intramembrane particles between the fractured plasma and granule membranes. However, as seen in thin sections, the granule membrane appears thinner than the plasmalemma (Figs. 12 and 17), and linear discontinuities in the fracture plane that might be junctions between plasma and granule membranes were occasionally found in the necks of opened granules (Fig. 9). The details of these junctions are seen with greater clarity and certainty, in thin sections, but in freeze-fracture views it is at least clear that such structures do not completely surround the necks of large pores.

Amebocytes Examined with Freeze-Substitution

The smooth contour of the plasmalemma of normal cells exhibited by freeze-fracture also characterized much of the cell surface in thin-section views. Postsubstitution hafnium staining also revealed a granular cytoplasm that, at the cell periphery, was interspersed with fibrous elements (Fig. 10). The granules at the cell periphery typically were separated from the plasmalemma by 0.2 μm at their closest approach (Fig. 11).

After endotoxin treatment, the plasmalemma buckled inward, narrowing the intervening band of cytoplasm until the dense lines of the granule and plasmalemmal trilaminar membranes became closely apposed except at points where granular cytoplasmic elements remained in the cleft. This apposition mandated a second inflection in the plasmalemma at the top of each inward bulge in order for it to conform to the convex shape of the granule; this shape paralleled that of the plasmalemmal pedestals seen with freeze-fracture (Figs. 5 and 12). However, actual contact of the apposed trilaminar membranes was difficult to observe in conventional electron microscope images. We had to tilt sections about the axis of the apposition to be certain that small regions of the apposition had formed

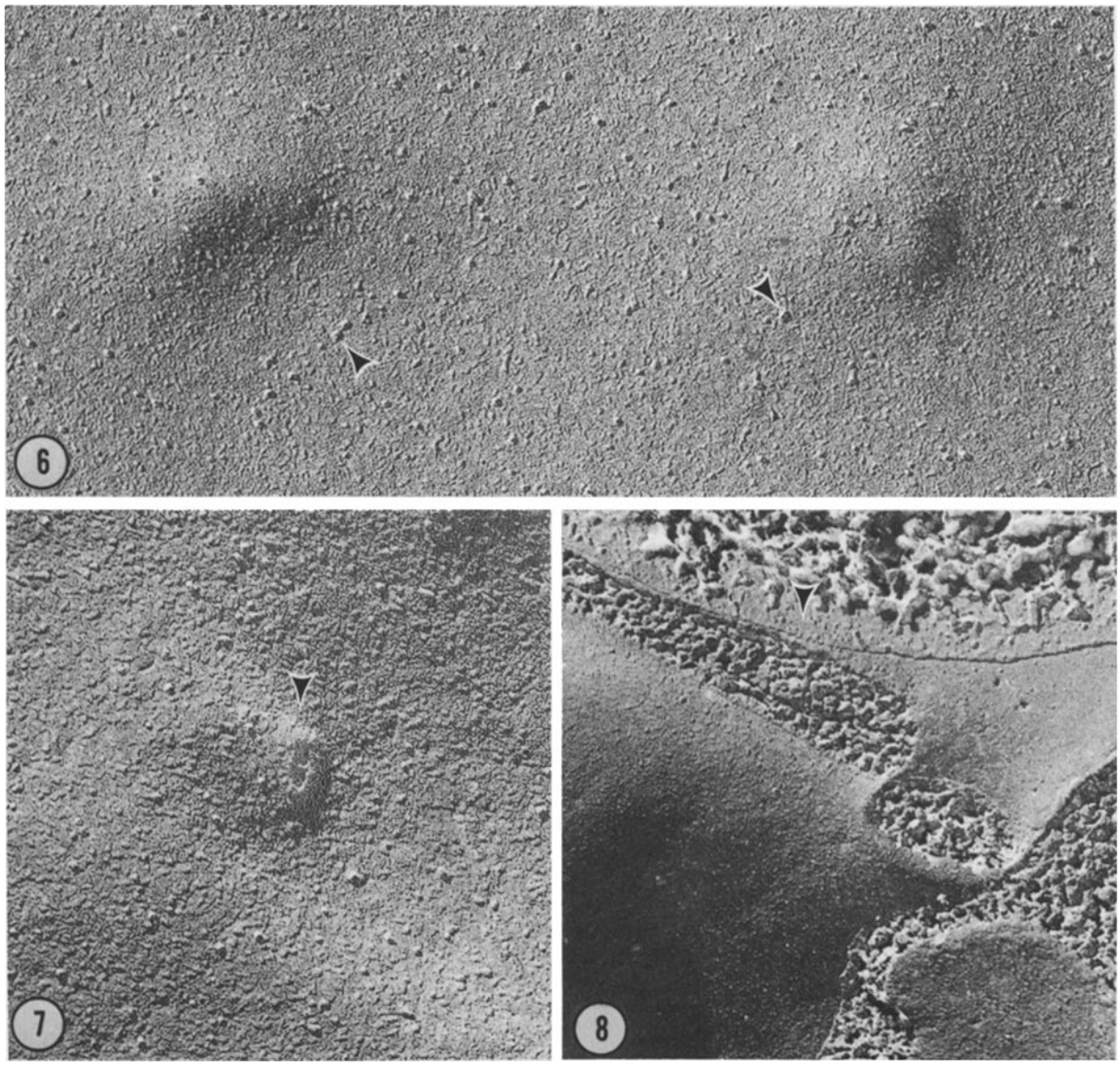

FIGURE 6 Pedestals on the E face of the plasma membrane of a stimulated amebocyte vary in their size and shape, perhaps representing stages in their formation. The concentration and distribution of the large particles on these pedestals are similar to those on the rest of the plasmalemmal E face (arrowheads). × 50,000.

FIGURE 7 Plasmalemmal E face, with a pedestal showing a small invagination of the plasmalemma (arrowhead), which might connect it to the granule interior. The distribution of large particles over the rest of the E face of the pedestal surface is the same as that over the rest of the plasmalemma. × 60,000.

FIGURE 8 Larger type of pore, typical of the period from 5 to 15 s after exposure to endotoxin, connecting the interior of a secretory granule with the plasmalemma. In contrast to the examples in Figs. 6 and 7, the P face of the plasmalemma is now shown (right). The pedestal has disappeared, perhaps engulfed in the widening pore, which may account for the long cross-fractured neck (just right of center) characteristic of granule openings at later stages. The granule E face is visible on the left of the neck. Blood plasma is seen at the top, and just below it a thin ridge of the external plasmalemmal surface (arrow) has been exposed by etching. × 50,000.

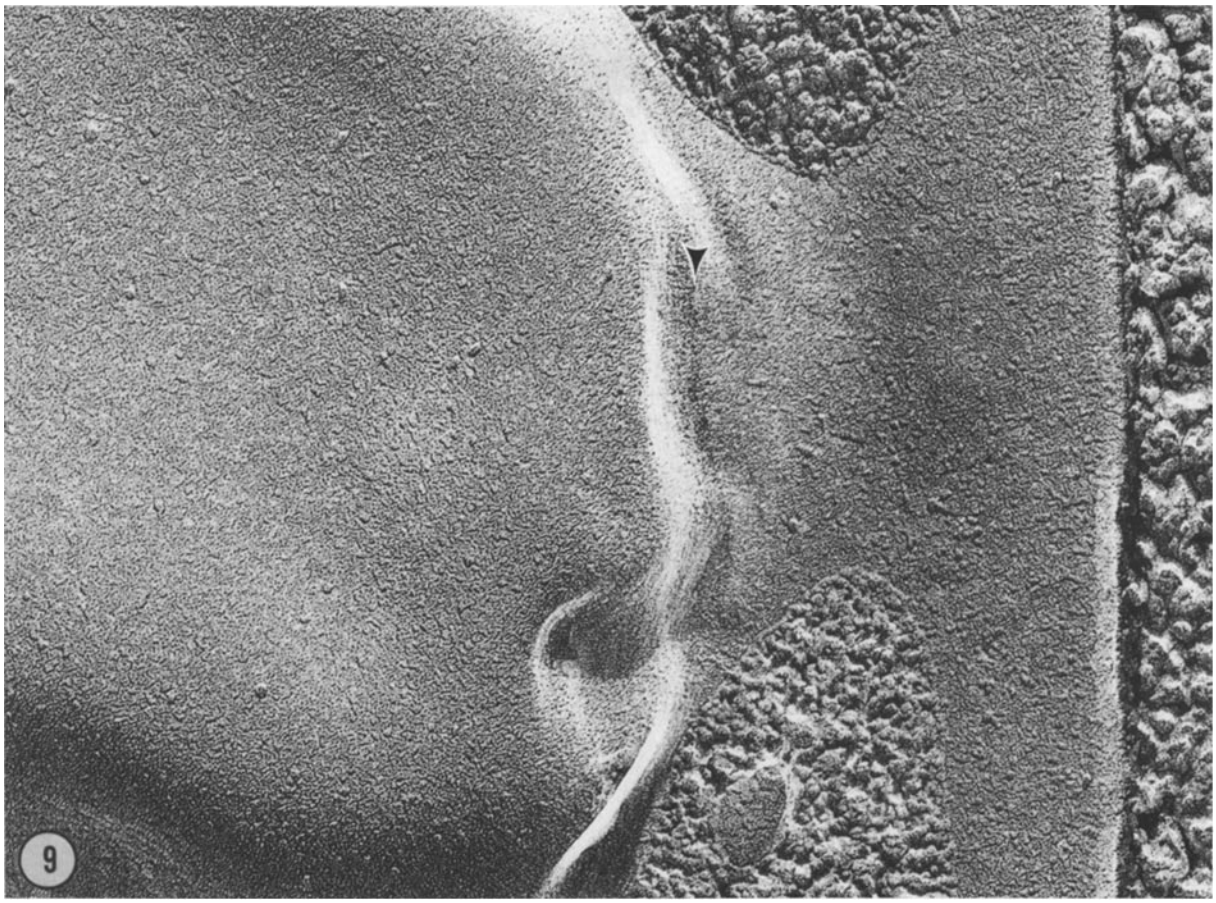

FIGURE 9 External fracture face of a secretory granule that has formed a large pore opening onto the plasmalemma. The distribution of intramembrane particles on the granule membrane E face (left) is similar to that on the plasmalemmal E face (right). A ridge in the neck of the open secretory granule (arrowhead) may represent the joint where the granule membrane originally joined the surface membrane. Just to the left of this point, the granule membrane is ruffled. The blood plasma around the amebocyte is exposed at the right, while cross-fractured cytoplasm is seen above and below the neck. × 130,000.

pentalaminar contacts (Figs. 12 and 13).

When each section of a series through a plasmalemmal pedestal was appropriately tilted, it became clear that several regions of punctate pentalaminar contacts are present in each apposition. However, no further thinning of these structures, nor any merging into larger areas of pentalaminar contact, was ever observed. Instead, membrane discontinuities interpreted to be small porelike openings were found at a very small proportion of these appositions. Because these openings were contained within one or two sections 45–50 nm thick, they were only clear to us in stereo views (Fig. 13). The contour of the membrane forming the walls of a pore was inferred from continuities of the dense and lucent laminas of the plasmalemma with those of the apposed granule membrane.

In conformity with the results from freeze-fracture, wider and presumably older openings were far more frequent than small pores. Remnants of the plasmalemmal depressions were easily recognized at the mouths of some of the smaller openings of this type (Fig. 14). The contour of the luminal neck at later openings was usually gently curved, but sometimes a sharper contour, actually a corner, was found at smaller ones. These corners did not surround the opening and appeared to be an end-to-end joint between the thinner granule membrane and the thicker plasmalemma (Figs. 14 and 17). These joints were even found occasionally at places where the two component membranes no longer made a corner but had rotated into the smooth, gently curved contour typical of the necks of granule openings (Fig. 17). We wish to stress that these sharp transitions were not found in all, or even most, granule necks. Where they were absent, the plasma membrane gradually assumed the thickness of the granule membrane (Fig. 16).

The granule membrane just below where it joined the plasmalemma was usually wrinkled (Fig. 14). These wrinkles are probably not an artifact of freeze-substitution because they were also recognized in freeze-fracture replicas (Fig. 9). Some wrinkles terminated in small peaks that protruded into the cytoplasm surrounding the granule neck. These peaks were associated with cytoplasmic densities, which suggested a cytoplasmic connection with these regions of the granule membrane.

A change in the appearance of the granule contents accompanied the development of exocytotic pores. The earliest change, associated with the initial formation of small pores in the few available examples, consisted of a separation between the granule core and its membrane, leaving an intervening clear crescent (Fig. 13). Even though pores were accompanied by clear spaces, these spaces also appeared at appositions where it was unknown whether or not a pore had formed. In fact, it was too difficult to find clear examples of early pores in serial sections to be able to conclude that clear spaces never occur before a pore has formed. At larger pores the clear space advanced in conjunction with the appearance of the wrinkled regions of the plasmalemma described above (Fig. 14). As pore expansion continued, the clear space moved to circumscribe

the granule core, ahead of the inward-moving front of dissolution of the granule contents (Figs. 15–17).

The dissolution of the granule core, which contains the blood clotting proteins (21), was arrested by quick-freezing, and the substructure of the dissolving contents was clearly delineated by the hafnium block stain. This dissolution progressed inward from the original pore in a wavelike fashion (Figs. 14 and 15). The granule core had no clearly delineated substructure in resting cells nor in stimulated cells ahead of the front of granule dissolution. The first change after a pore formed was the darkening (with hafnium staining) of the granule contents as they broke up into columns of small corpuscles 50–100 nm in diameter oriented perpendicular to the wave of dissolution (Fig. 15). These corpuscles left the interior of the granule

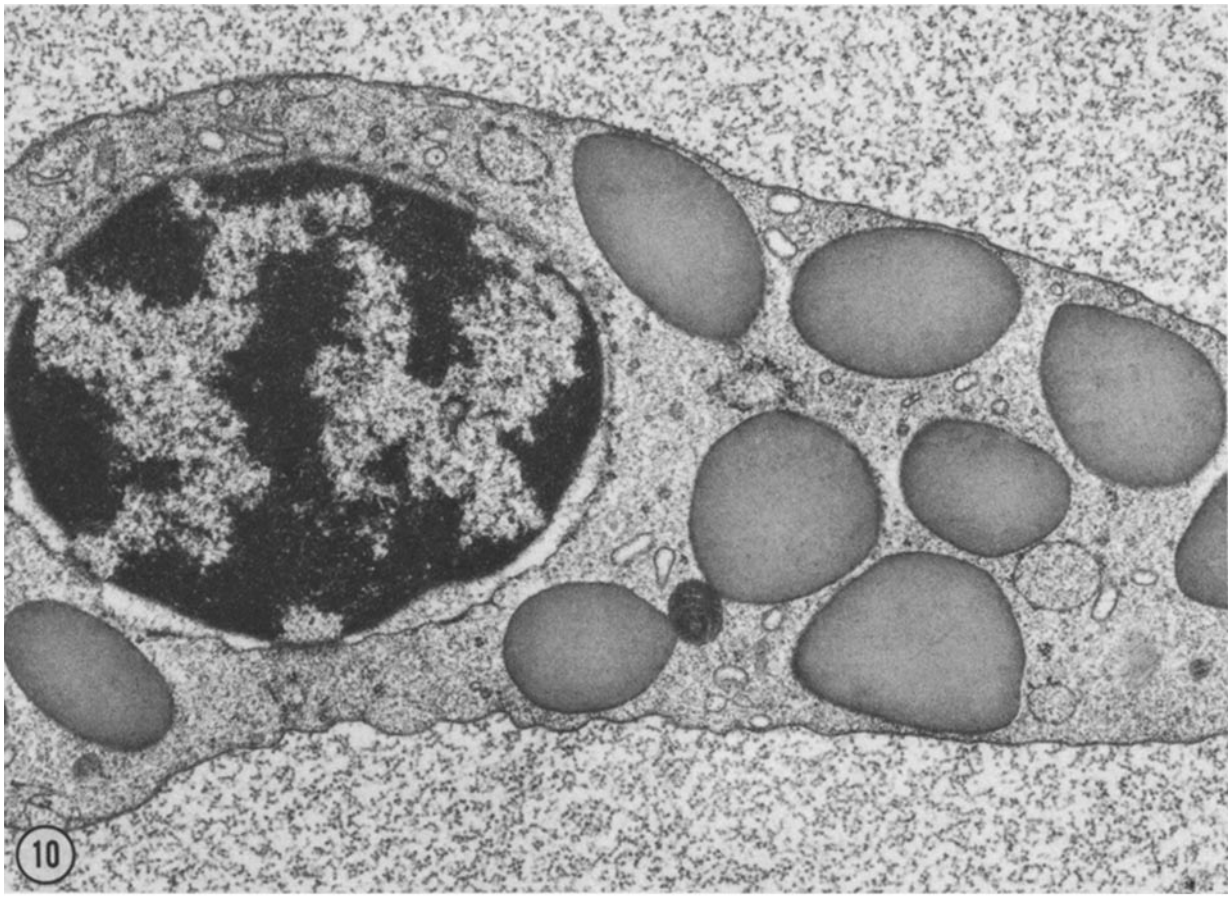

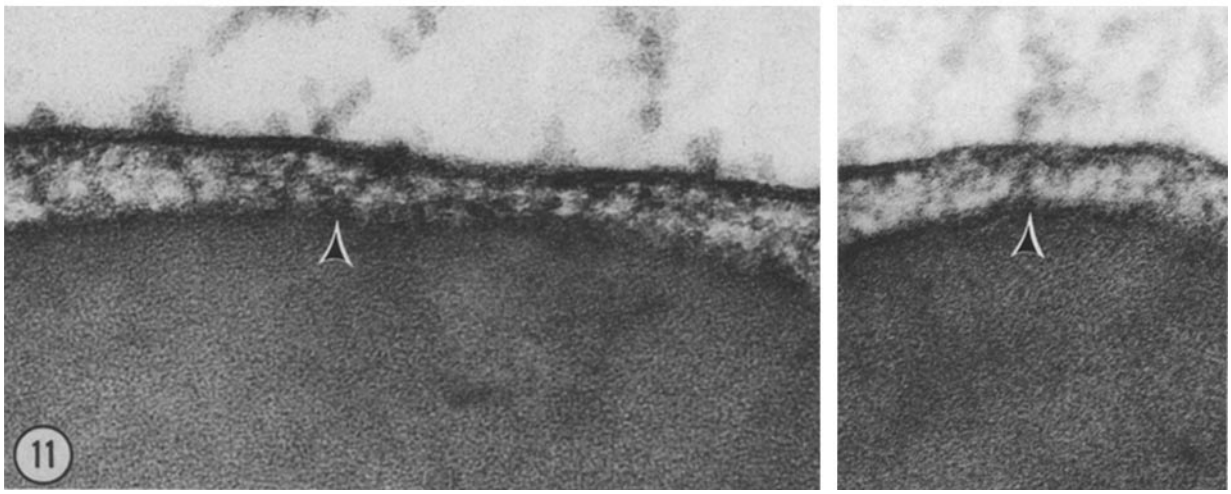

FIGURE 10 Freeze-substituted amebocyte from an unstimulated preparation. Secretory granules are separated from the plasma membrane by narrow gaps because the plasma membrane is not bulging in and contacting them. The plasmalemmal infoldings seen along the bottom edge of this cell are actually parallel ridges, which in freeze-fracture replicas together clearly differentiated from the stimulation-dependent membrane bulges. × 21,000.

FIGURE 11 Relationship of a granule membrane to the plasmalemma that is typical of the closest encounters found in resting cells. Filamentous densities bridging this gap (arrowhead) are found in some planes of section through these appositions. × 175,000.

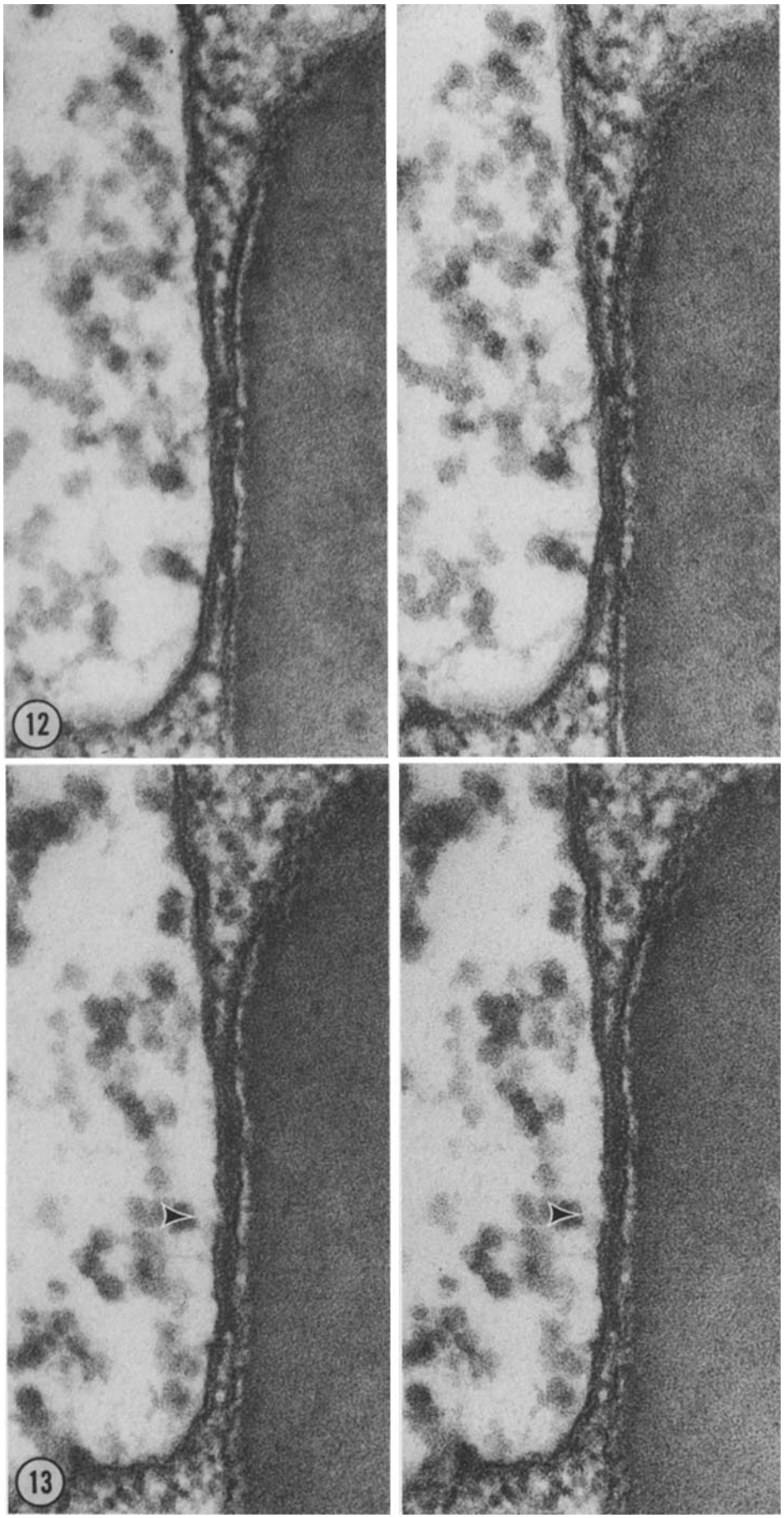

FIGURES 12 AND 13 Stereo views from a series of sections through a pedestal formed 5 s after application of endotoxin. Fig. 12 shows an example of an intermembrane contact or fusion at an apposition between a plasma and granule membrane. In an adjacent section (Fig. 13) the membranes of the surface and the granule have formed an end-to-end joint (fission), so a minute pore now connects the granule interior with the outside of the cell (arrowhead). Because this pore is smaller than the section thickness, it is only appreciated in stereo views. Block stained with uranyl acetate in methanol. × 200,000.

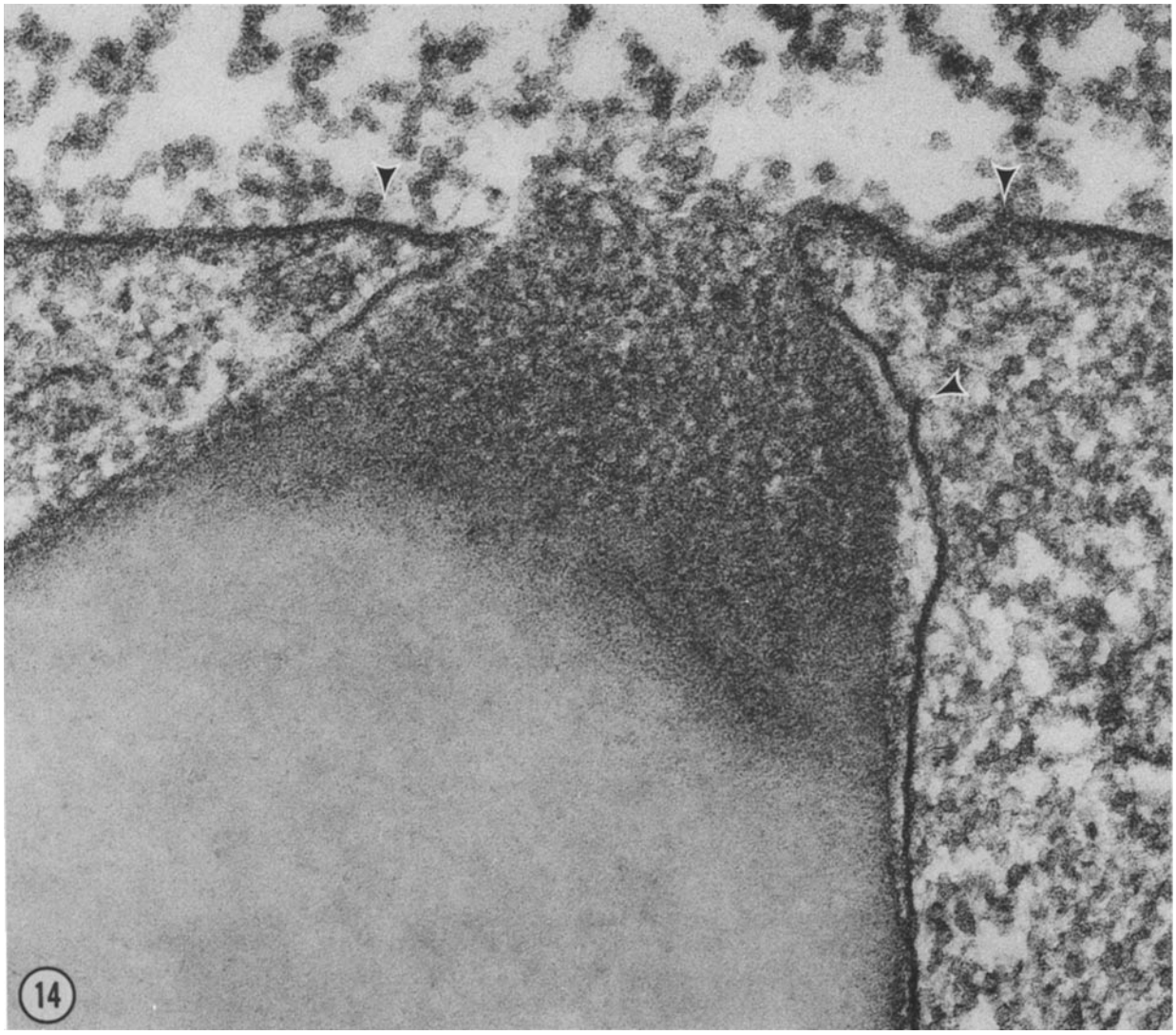

FIGURE 14 Large pore connecting a secretory granule to the plasmalemma at 5 s after application of endotoxin. Shoulders of the original pedestal are still apparent (between arrowheads at top). The pore neck, at left, consists of a sharp corner that may represent the original joint between the plasmalemma and the granule membrane. The lateral granule membrane is separated by a clear space from the granule contents and is ruffled apically; some of these ruffles terminate as sharp peaks (lower arrowhead at right). The morphological changes in the granule contents are stratified in a way that suggests a progressive dissolution of the granule contents, beginning at the original pore. × 48,000.

through the exocytotic opening, leaving behind a fine web of material that may be the beginning of a clot, or a matrix material covered over in the intact granule by denser structures (Fig. 16).

The dissolution of the core thus proceeded in an orderly sequential fashion from the pore inwards, so it could be regarded as a "clock" telling the age of an open granule. In fact, the necks of open granules with approximately half their contents dissipated were smoothly contoured (Fig. 16), whereas those that had more of their core intact often had sharper corners at some of the edges of the pore and clear remnants of the plasmalemma depressions (Fig. 14). The actual time for dissipation of granule contents may be estimated from movies of the live cells to be ~0.1–0.5 s (unpublished film by Jack Levin, Department of Hematology, Johns Hopkins Medical School), which provides a rough calibration of this clock, particularly if the flashes of light that accompany exocytosis result from diffraction by the highly ordered columns of dissipating granule content.

Cytoplasmic Structure

The invagination of the surface membrane to contact the peripheral granules suggested the presence of a contractile system that would pull in on the surface membrane. Freeze-etch views of the cytoplasm between the plasmalemma and granules revealed pieces of filamentous structures in the spaces between granules and the adjacent plasma membrane, but the plethora of other cytoplasmic elements made it difficult to delineate the connections of these filamentous structures. In freeze-substituted amebocytes, dense, elongated structures ~5–8 nm in diameter often crossed the space between the plasmalemma and the facing surface of the granule membrane in unstimulated cells; these were seen more clearly after uranyl acetate block-staining where other cytoplasmic elements were more lightly stained (Fig. 11). Similar filamentous structures persisted throughout release at the perimeter of exocytotic openings, where they bunched as the granule opening widened (Figs. 16 and 18).

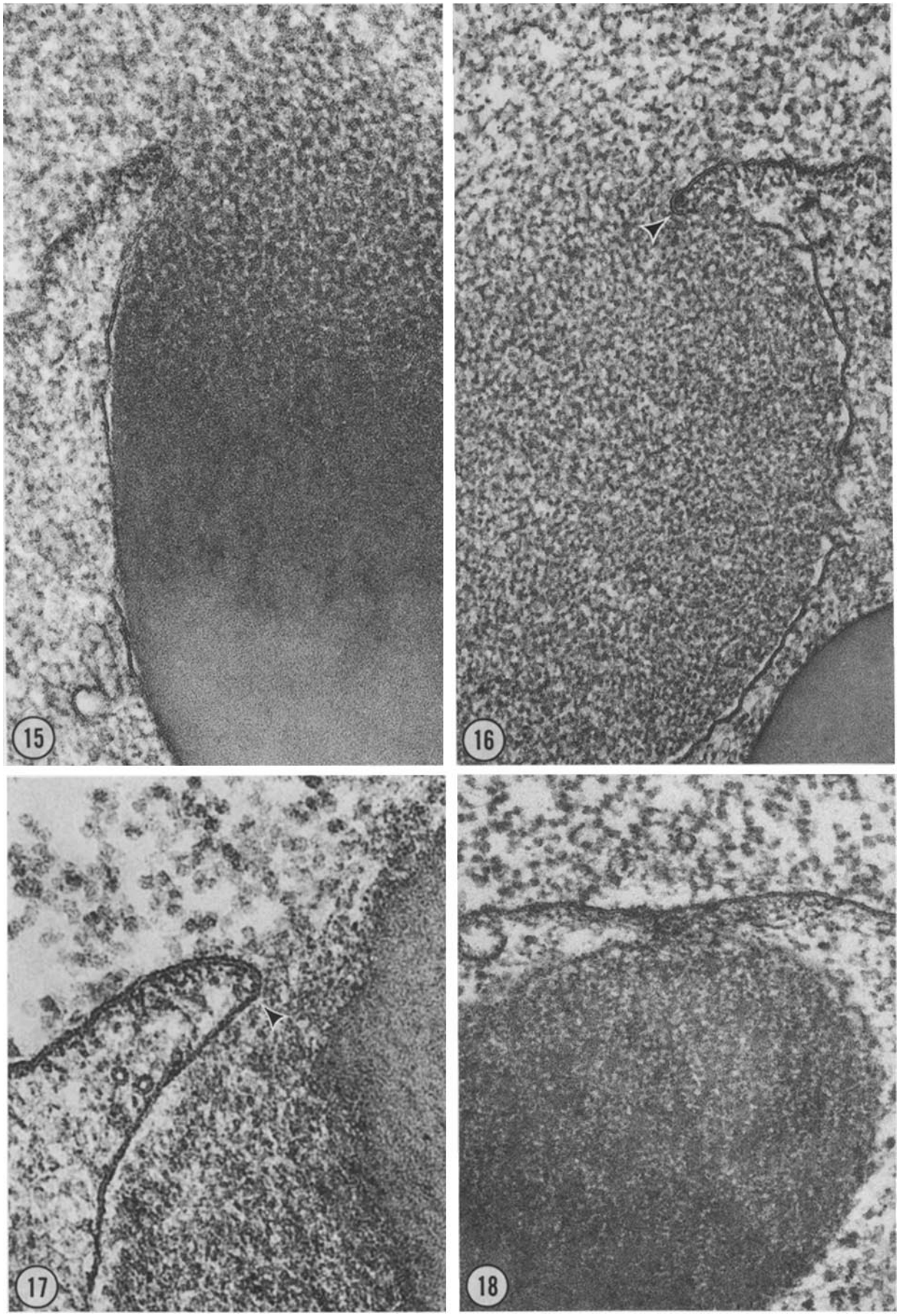
15
16
17
18

Another possible manifestation of a tension-generating mechanism between the granule and plasma membranes may be the cusplike folds in the necks of openings described above (Fig. 14). Again, individual filaments could seldom be followed in their entirety, particularly in hafnium-stained cells, because of the granular nature of the intervening cytoplasm. Therefore we are unable to present a complete three-dimensional picture of these filaments or their displacements during successive stages in the release of the secretory granules.

In an attempt to determine whether any of the structural changes that accompany secretion might depend on actin (36), we examined the effect of cytochalasin D on endotoxin-induced degranulation in living cells and on the formation of pedestal-like depressions in the plasmalemma of freeze-fractured cells. Cytochalasin D was used because it is more specific for actin filaments in that, unlike cytochalasins A and B, it does not inhibit glucose uptake (14, 20) or affect surface sulfhydryl groups (23). After a brief treatment (1–2 min), cytochalasin D (10 μg/ml) inhibited attachment to the glass substrate as well as flattening and motility of the amebocytes, but it did not prevent degranulation induced by endotoxin (Figs. 19 and 20). Similarly, the formation of the plasmalemmal depressions was not impaired by cytochalasin D even after 10 min of cytochalasin D exposure before endotoxin exposure. The lack of an effect on amebocytes by cytochalasin D does not eliminate the possibility that actin filaments are involved in the initiation of exocytosis, because cytochalasins D and E disrupt actin during the polymerization of G-actin monomers (1). Only those filaments that are undergoing cycles of polymerization-depolymerization might be affected. Thus, our results do not rule out the possibility that exocytosis in amebocytes depends on an unusually stable form of cytoplasmic actin.

Damaged Cells

A few cells in some experiments showed a set of morphological changes that we took to be indicative of damage and, therefore, not part of the normal sequence of exocytosis. The plasmalemma of these cells was ruptured, and secretory granules, with or without limiting membranes, were often extruded. The contents of all granules within these cells had a striking substructure, which resembled the earliest changes that occur during granule dissolution, but the distribution of these changes differed from normal in that the whole granule content was uniformly affected. Granules showing these changes occasionally formed five-layered contacts with the cell surface covering up to one-third of the granule diameter. Images of exocytotic openings, where granule contents were partially extruded without further dissolution, or even whole extruded granules were also found occasionally around such cells.

That most of these changes should be attributed to mechanical damage during freezing is suggested by the following observations. When a drop of amebocyte blood was frozen against the cold block, it had a flat surface with an area approaching that of the filter paper support. For the drop to assume this shape, lateral flow from the center of the drop to its edges must occur after contact with the cold block. When drops exceeded a volume of 10 μl in our system, strands of blood even extended beyond the edge of the central paper disk, suggesting that a splash occurred on contact with the cold block. It was in the lateral regions of the frozen droplet, particularly when splashing occurred, that cells with the changes described above were more frequently found. As expected, these changes tended to affect large groups of cells away from the original center of the drop of blood, so regions sideration. The distorted edges of frozen drops may explain the with groups of these abnormal cells were excluded from conelliptical deformation or stretching of microvilli and exocytotic structures recently described (31) for quick-frozen sea urchin eggs (3).

DISCUSSION

We have presented freeze-fracture and thin-section views of the initial stages of exocytosis in *Limulus* amebocytes. These views, which are based on rapid-freezing synchronized with stimulation by endotoxin, establish a predictable sequence of morphological changes that accompany exocytosis of the secretory granules lying at the periphery of this cell. This sequence of morphological changes is the basis of a hypothetical scheme of secretory granule exocytosis presented in Fig. 21. In this scheme, exocytosis begins when the plasmalemma buckles into apposition with a secretory granule. One of the several punctate pentalaminar junctions that form at each apposition is then rearranged into an equally small exocytotic pore. This pore widens quickly as the granule contents dissolve and diffuse into the extracellular space. According to this scheme, only focal regions of the apposed granule and plasma membranes are involved in initiating an exocytotic pore.

These results and conclusions differ in several respects from previous ideas about the beginning of exocytosis. The most important differences concern the events surrounding the initial apposition of the secretory granule with the plasma membrane and the subsequent formation of an exocytotic pore. We did not see exclusion of membrane particles from these regions of apposition between the plasmalemma and granule membranes nor the appearance of extensive pentalaminar junctions between the two membranes. Successive elimination of membrane layers was also never seen at those punctate pentalaminar contacts that did form. Current concepts of membrane fusion must therefore be reexamined in the context of these discrepancies.

Clearing of intramembrane particles at sites of exocytosis was first seen in mast cells (2, 5), and later in pancreatic beta cells (25), neurohypophysis (41), fungal spores (32), and myo-

FIGURES 15–18 Later stages of granule exocytosis at 5–15 s after exposure to endotoxin. The necks of these pores are rounded and may be bounded by a sharp (Fig. 17, arrowhead) or a gradual (Fig. 16, arrowhead) transition between the granule and the surface membrane. Submembrane filamentous densities concentrated in the cytoplasm around these necks (Figs. 16 and 17) fan out and mingle with surrounding subplasmalemmal filaments (*en face* view; Fig. 18). Various stages of granule dissolution are shown; both the stratification of granule contents typical of the partially expanded contents (Figs. 15, 17, and 18) and the matrix or clot material left behind after the dense contents have left the granule (Fig. 16) can be seen. The plane of section in Fig. 18 is favorable to show that the dense granule contents form columns perpendicular to the plasmalemma during early stages of dissolution. Serial sections showed that this granule was connected to the plasmalemma by a large pore. Figs. 15 and 16, × 80,000; Fig. 17, × 45,000; Fig. 18, × 72,000.

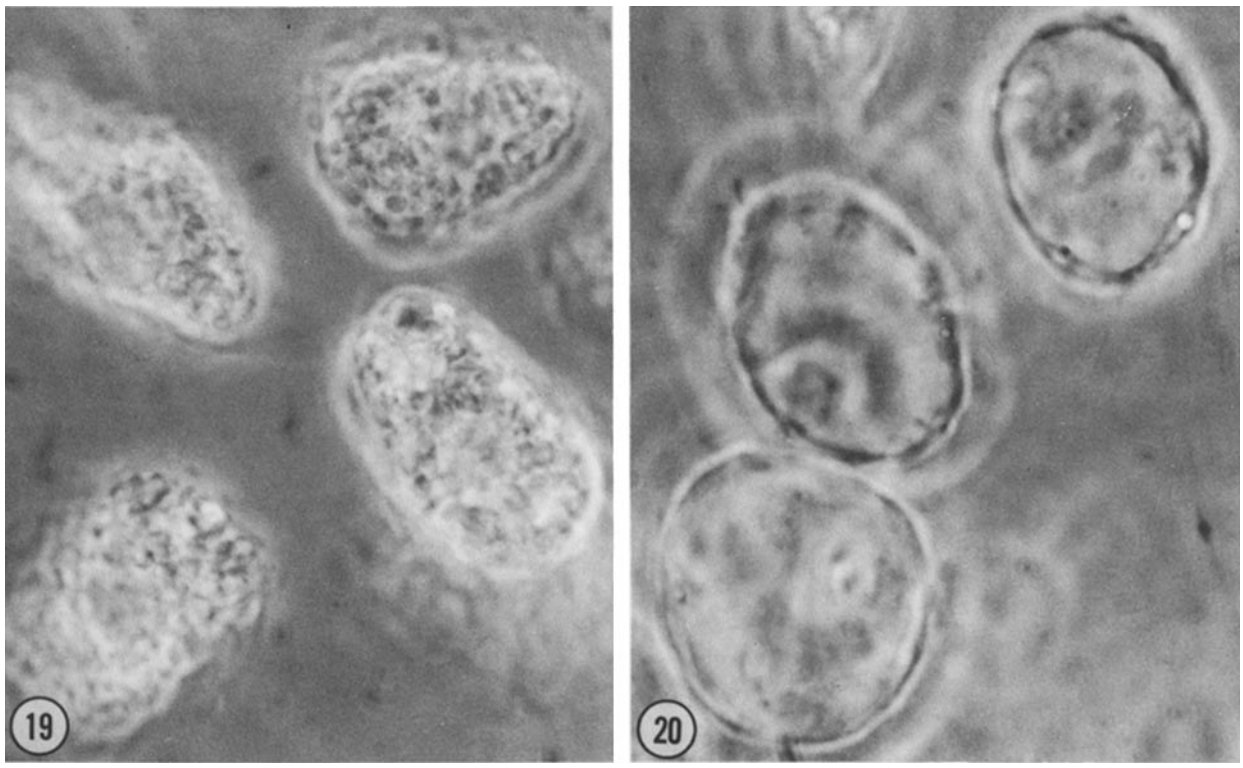

FIGURES 19 AND 20 After exposure to cytochalasin D, amebocytes round up and do not stick to a glass substrate (Fig. 19). Nevertheless, treated amebocytes still discharge their secretory granules upon exposure to endotoxin (Fig. 20). × 1,700.

tubes (13). This seemingly universal observation provided a basis for assuming that membrane fusion involves only the lipid portion of the contacting membranes. Indeed, detailed explanations of intramembrane particle clearing have been proposed (9) as well as schemes for the molecular rearrangement of membrane lipids to explain the formation of exocytotic pores (15, 19, 22, 31, 37). However, it has recently been recognized that particle clearing at exocytotic sites can also be an artifact of the glycerination conventionally used before freeze-fracture (3), although amebocytes and pancreatic acinar cells (40) do not appear to be subject to this artifact. The present results are therefore not pertinent to the issue of whether particle clearing at exocytotic sites is an artifact of tissue preparation, but they do suggest that this phenomenon is not universally required for exocytosis.

Thin sections through granule-plasmalemma appositions in conventionally prepared tissues have generally revealed pentalaminar junctions between the plasmalemma and granule membrane that encompass most of their apposition (13, 16, 25). In addition, trilaminar or unilaminar diaphragms, believed to result from successive fusion of the components of these pentalaminar junctions, have also been observed (13, 30). We do not find these structures in amebocytes, though the punctuate pentalaminar contacts captured by rapid-freezing might be regarded as smaller versions of the extensive pentalaminar contact seen at granule-plasmalemmal appositions in other secretory cells prepared by chemical fixation. Alternatively, the punctate contacts seen after rapid-freezing may be basically different from those seen in other cells prepared with fixatives. In either instance, our results suggest that pore formation is a direct, but infrequent, outcome of the formation of a punctate pentalaminar contact. The time-course of the transition from contact to pore as well as the necessity of forming an intermediate diaphragm is uncertain. It remains unclear whether membrane fusion and fission in amebocytes can be regarded as sequential and distinguishable.

The steps leading to release of a secretory granule must depend on the application of various forces at each stage of exocytosis. Our results suggest that these forces might be exerted by a juxtagranular filamentous network and osmotic gradients between the granule and the outside of the cell; other ideas about the forces leading to fusion at five-layered appositions are not ruled out (8). A network of filamentous structures connects the plasmalemma with some, but possibly not all, of the peripheral granules in resting cells. Ideally, these filamentous structures are deployed to pull the plasmalemma into apposition with secretory granules and to produce the ruffles that appear in lateral regions of the granule membrane after exocytosis begins. Later, filaments are bunched around the widening mouth of the exocytotic pore and might be contributing to the slowing in the rate of expansion of these pores late in exocytosis. Our results do not rule out the opposite possibility that the filaments obstruct exocytosis in resting cells, so that they must be removed before exocytosis begins.

The formation of an exocytotic pore at or near a punctate pentalaminar junction may also require a locally applied force. It is difficult to picture how the filaments, even if they are contractile, could apply this localized force. A better possibility is an intragranular osmotic pressure that would depend on an osmotic gradient, at this point hypothetical, between the granular interior and the extracellular space. This idea is supported by recent studies of artificial vesicle fusion with artificial bilayers, which have shown that membrane fusion requires an osmotic gradient (6, 42). The need and the means for generating osmotic gradients in secretory cells have been appreciated for some time (33).

The thin rim of clear space that appears between the granule membrane and its contents in amebocytes can be attributed to a water influx resulting from an osmotic gradient between the granule interior and the extracellular environment. Similar clear spaces in aggregated chromaffin granules have also been attributed to osmotically driven water influxes (8). However, we were not able to determine whether these clear spaces precede or follow pore formation and thus whether osmotic forces initiate pore formation or only act immediately afterwards, during the radial expansion of the pore. It is clear, however, that much of the subsequent widening of the pore precedes the morphological changes that we interpret as dissolution of the granule contents.

A rapid expansion of the small pores is inferred from their very low frequencies, which may explain why the various stages of granule core dissolution and release are not captured by conventional methods of fixation. The actual release of the core material occurs from large pores, starting with the dissolution of the surface layer exposed by the rapid expansion of the pore. Successive layers then dissolve and the dissolved granule contents more out of the open granule cavity. Expulsion of intact granule cores as seen in mast cells (16) and the neurohypophysis (41) may therefore be an artifact of aldehyde fixation or cell damage.

The joint that persists between the granule and plasma membrane in the necks of large pores suggests that mixing of granule with plasma membrane may be slower than expected from considerations of lipid fluidity. This limitation could be attributable to cross-linking between membrane components or between membrane and extramembrane components, or to decreased lipid fluidity. Freeze-fracture views do not reveal changes in the distribution of membrane particles at the granule

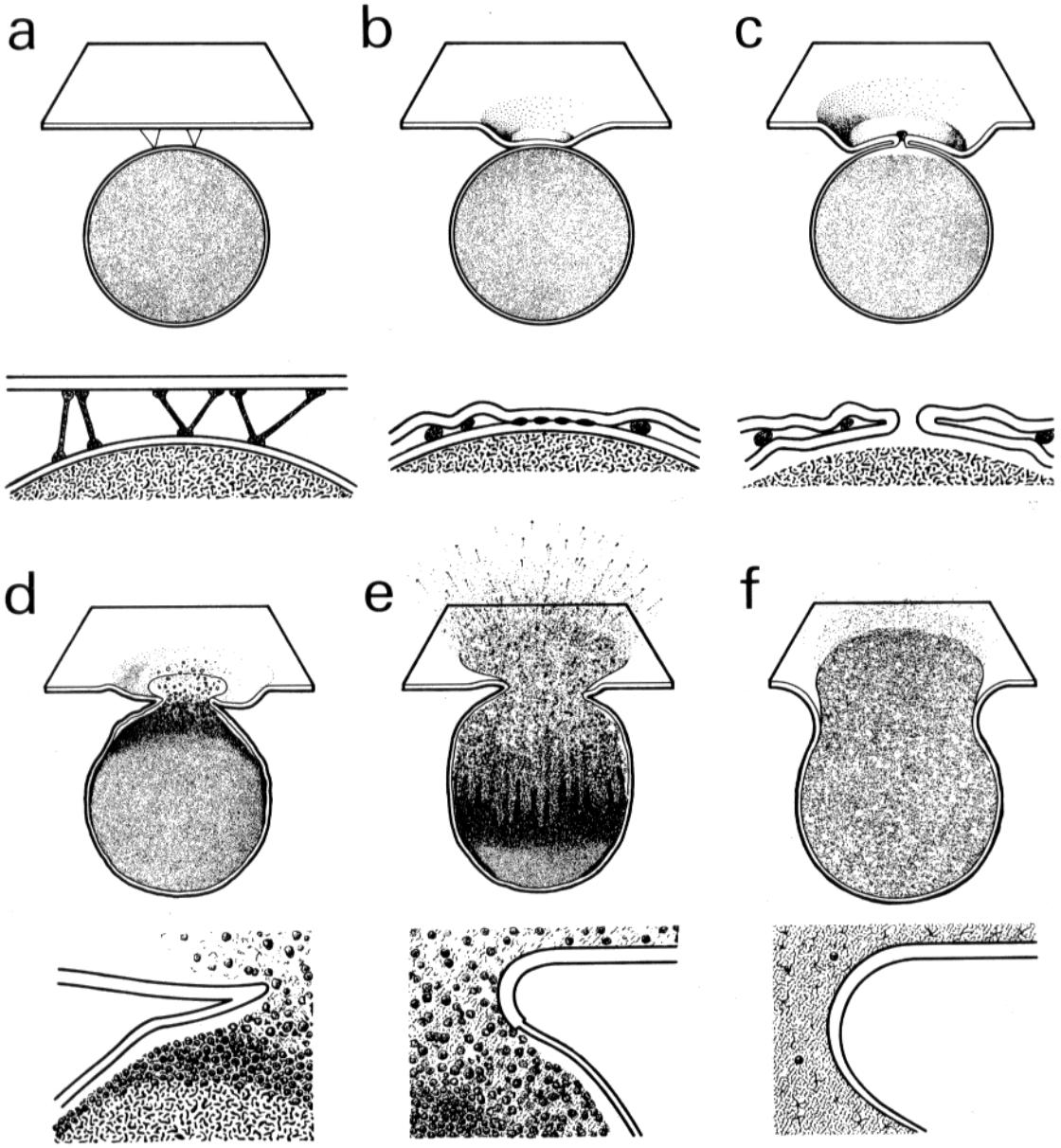

FIGURE 21. Hypothetical sequence of the morphological changes that underlie exocytosis of secretory granules at the periphery of *Limulus* amebocytes. Stage a typifies unstimulated cells; b and c, cells stimulated for 1–5 s; d, cells stimulated for 5–10 s; and e and f, cells stimulated for 10–15 s. These times, combined with reasonable expectations about the course of exocytosis, are the basis for fitting the morphological changes described here into a sequence. The blood space around the amebocyte is at the top of each drawing.

neck but suggest that the sharp transitions do not encircle the necks of large pores. If the original joint between the granule membrane and plasmalemma is relatively stable, as discussed above, it must break up to admit additional membrane as the pore expands. Whether this added membrane comes from the plasmalemma, granule membrane, or both is unclear.

We thank Dr. Harvey Pollard for suggesting the amebocyte preparation to us. We also are grateful to Bryan Schroeder for his photographic assistance, to Ruth Campbell at the Marine Biological Laboratory for typing, to Sandra Cotter for editorial assistance and typing, to Bob Golder at the Marine Biological Laboratory for drawing Fig. 21, and to Dr. David Shotton for his careful review of the manuscript.

Received for publication 29 August 1980, and in revised form 10 February 1981.

REFERENCES

1. Brown, S. S., and J. A. Spudich. 1979. Cytochalasin inhibits the rate of elongation of actin filament fragments. *J. Cell Biol.* 83:657–662.
2. Burwen, S. J., and B. Satir. 1977. A freeze-fracture study of early membrane events during mast cell secretion. *J. Cell Biol.* 73:660–671.
3. Chandler, D. E., and J. E. Heuser. 1979. Membrane fusion during secretion. Cortical granule exocytosis in sea urchin eggs as studied by quick freezing and freeze-fracture. *J. Cell Biol.* 83:91–108.
4. Chandler, D. E., and J. E. Heuser. 1980. Arrest of membrane fusion events in mast cells by quick freezing. *J. Cell Biol.* 86:666–674.
5. Chi, E. Y., D. Lagunoff, and J. K. Koehler. 1976. Freeze-fracture study of mast cell secretion. *Proc. Natl. Acad. Sci. U. S. A.* 73:2823–2827.
6. Cohen, F. S., J. Zimmerberg, and A. Finkelstein. 1980. Fusion of phospholipid vesicles with planar phospholipid bilayer membranes. II. Incorporation of a vesicular membrane marker into the planar membrane. *J. Gen. Physiol.* 75:251–270.
7. de Duve, C. 1963. Endocytosis. *CIBA Found. Symp.* 126.
8. Edwards, W., J. H. Phillips, and S. J. Morris. 1974. Structural changes in chromaffin granules induced by divalent cations. *Biochim. Biophys. Acta.* 356:164–173.
9. Gingell, D., and L. Ginsberg. 1978. Problems in the physical interpretation of membrane interaction and fusion. *In* Membrane Fusion. G. Poste and G. L. Nicholson, editors. Elsevier North-Holland, Inc., New York. 792–829.
10. Heuser, J. E., and T. S. Reese. 1974. Morphology of synaptic vesicle discharge and reformation at the frog neuromuscular junction. *In* Synaptic Transmission and Neuronal Interaction. M. V. L. Bennett, editor. Raven Press, New York. 59–77.
11. Heuser, J. E., T. S. Reese, M. J. Dennis, Y. Jan, L. Jan, and L. Evans. 1979. Synaptic vesicle exocytosis captured by quick-freezing and correlated with quantal transmitter release. *J. Cell Biol.* 81:275–300.
12. Heuser, J. E., T. S. Reese, and D. M. D. Landis. 1974. Functional changes in frog neuromuscular junctions studied with freeze-fracture. *J. Neurocytol.* 3:109–131.
13. Kalderon, N., and N. B. Gilula. 1979. Membrane events involved in myoblast fusion. *J. Cell Biol.* 81:411–425.
14. Kletzien, R. J., J. F. Perdue, and A. Springer. 1972. Cytochalasin A and B. Inhibition of sugar uptake in culture cells. *J. Biol. Chem.* 247:2964–2966.
15. Lau, A. L. Y., and S. I. Chan. 1974. Nuclear magnetic resonance studies of the interaction of alamethicin with lectin bilayer. *Biochemistry.* 13:4942–4948.
16. Lawson, D., M. C. Raff, B. Gomperts, C. Fewtrell, and N. B. Gilula. 1977. Molecular events during membrane fusion: a study of exocytosis in rat peritoneal mast cells. *J. Cell Biol.* 72:242–259.
17. Levin, J., and F. B. Bang. 1964. The role of endotoxin in the extracellular coagulation of *Limulus* blood. *Bull. Johns Hopkins Hosp.* 115:265–274.
18. Levin, J., and F. B. Bang. 1964. A description of cellular coagulation in the *Limulus*. *Bull. Johns Hopkins Hosp.* 115:337–345.
19. Lucy, J. A. 1970. The fusion of biological membranes. *Nature (Lond.).* 227:814–817.
20. Mousa, G. Y., J. R. Trevithick, J. Bechberger, and D. G. Blair. 1978. Cytochalasin D induces the capping of both leukemia viral proteins and actin in infected cells. *Nature (Lond.).* 274:808–809.
21. Murer, E. H., J. Levin, and R. Holme. 1975. Isolation and studies of the granule of the amebocytes of *Limulus polyphemus*, the horseshoe crab. *J. Cell. Physiol.* 86:533–542.
22. Neher, E. 1974. Asymmetric membranes resulting from the fusion of two black lipid bilayers. *Biochim. Biophys. Acta.* 373:327–336.
23. Nemeth, E. F., and W. W. Douglas. 1978. Effects of microfilament-active drugs, phalloidin and the cytochalasins A and B, on exocytosis in mast cells evoked by 48/80 or A23187. *Naunyn-Schmeideberg's Arch. Pharmacol.* 302:153–163.
24. Orci, L., and A. Perrelet. 1978. Ultrastructural aspects of exocytosis membrane fusion. *In* Membrane Fusion. G. Poste and G. L. Nicolson, editors. Elsevier North-Holland, Inc., New York. 629–656.
25. Orci, L., A. Perrelet, and D. S. Friend. 1977. Freeze-fracture of membrane fusions during exocytosis in pancreatic B-cells. *J. Cell Biol.* 75:23–30.
26. Ornberg, R. L., and T. S. Reese. 1979. Early stages of exocytosis captured by rapid-freezing. *Neurosci. Abstr.* 4:247.
27. Ornberg, R. L., and T. S. Reese. 1979. Artifacts of freezing in *Limulus* amebocytes. *In* Freeze Fracture: Methods, Artifacts, and Interpretation. J. E. Rash and C. S. Hudson, editors. Raven Press, New York. 89–98.
28. Palade, G. E. 1959. Functional changes in the structure of cell components. *In* Subcellular Particles. T. Hayashi, editor. Ronald, New York. 64–80.
29. Palade, G. E. 1975. Intracellular aspects of protein synthesis. *Science (Wash. D. C.).* 189: 347–358.
30. Palade, G. E., and R. R. Bruns. 1968. Structural modulations of plasmalemmal vesicles. *J. Cell Biol.* 37:633–648.
31. Pinto da Silva, P., and B. Kachar. 1980. Quick freezing vs. chemical fixation: capture and identification of membrane fusion intermediates. *Cell Biol. Int. Rep.* 4:625–640.
32. Pinto da Silva, P., and M. L. Nogueira. 1977. Membrane fusion during secretion: a hypothesis based on electron microscopy observation of *Phytophthora palmivora* zoospores during encystment. *J. Cell Biol.* 73:161–181.
33. Pollard, H. B., C. Pazoles, C. Creutz, and O. Zindler. 1979. The chromaffin granule and possible mechanisms of exocytosis. *Int. Rev. Cytol.* 58:159–197.
34. Pollard, H. B., K. Tack-Goldman, G. J. Pazoles, C. E. Creutz, and N. Raphael-Shusman. 1977. Evidence for control of peratoxin secretion from human platelets by hydroxyl ion transport and osmotic lysis. *Proc. Natl. Acad. Sci. U. S. A.* 74:5295–5299.
35. Prosser, C. L., editor. 1973. Comparative Animal Physiology. 3rd ed. W. B. Saunders Company. Philadelphia.
36. Rolich, P. 1975. Membrane-associated actin filaments in the cortical cytoplasm of the rat mast cell. *Exp. Cell Res.* 93:293–298.
37. Satir, B., C. Schooley, and P. Satir. 1973. Membrane fusion in model systems. Mucocyst secretion in *Tetrahymena*. *J. Cell Biol.* 56: 153–176.
38. Smith, J., and T. S. Reese. 1980. Use of aldehyde fixatives to determine the rate of synaptic transmitter release. *J. Exp. Biol.* 89:19–29.
39. Smith, U., D. S. Smith, H. Winkler, and J. W. Ryan. 1973. Exocytosis in the adrenal medulla demonstrated by freeze-etching. *Science (Wash. D. C.).* 179:79–82.
40. Tanaka, Y., P. de Camilli, and J. Meldolesi. 1980. Membrane interactions between secretory granules and plasmalemma in three exocrine glands. *J. Cell Biol.* 84:438–453.
41. Theodosis, D. T., J. J. Dreifuss, and L. Orci. 1978. A freeze-fracture study of membrane events during neurohypophysial secretion. *J. Cell Biol.* 78:542–553.
42. Zimmerberg, J., F. S. Cohen, and A. Finkelstein. 1980. Fusion of phospholipid vesicle with planar phospholipid bilayer membranes. I. Discharge of vesicular content across the planar membrane. *J. Gen. Physiol.* 75:241–250.